Wind induced motion on bundled conductors (Excluding ice galloping) Part A - Aeolian vibrations

Study Committee B2
resp.Working Group B2.46

Convenor: G.Diana, Secretary: H.J.Krispin

Members:

Jennifer Havel, Jason Huang, Julien Garnier, Sergey Kolosov, Jean Philippe Paradis, André Leblond , Chuck Rawlins, Umberto Cosmai, Pierre Van Dyke, Jean-Louis Lilien, Wolfgang Troppauer, Alessandra Manenti , Laura Mazzola, E. Ruggeri, Naji Sahlani, Douglas Proctor, Cécile Rozé, Marta Landeira, Sergio Thaddey, Claude Hardy, Ronald Tong, Bin Liu, A.Bhangor, A Vinogradov, T.Furtado, M.Araujo.

1. Introduction

Research conducted by Working Group B2.31 (formerly TF 1 of WG B2-11) and summarised in reports [1] [2] & [3], covers the modelling of Aeolian vibration of an undamped single conductor and of single conductor plus dampers. It has been shown that analytical methods based on the Energy Balance Principle (EBP in the following) and a shaker-based technology can provide a useful design tool for damping systems that protect a single conductor against Aeolian vibration.

One of the purpose of the present report is to evaluate the effectiveness of these methods for the design and/or verification of the damping system of conductor bundle spans with respect to Aeolian vibrations.

As in the case of the former papers, this report is based on an analysis of the available technology and on the results of benchmarks: an analytical-analytical benchmark and an analytical-experimental one are used for the evaluation relevant to Aeolian vibrations. The comparison between the analytical results produced by the different available models and the experimental one will help to understand the limitations and the usefulness of considered approach.

Field tests relevant to a 500 m quad bundle span equipped with ACSR Drake conductor and spacer-dampers have been selected as test case both for the analytical-analytical and analytical-experimental benchmark for the Aeolian vibrations evaluation. The selected case has a H/w parameter around 2000 m with respect to the safe design tension requirements according to [4] that is 2500 m.

It must be pointed out that EBP based methods do not simulate the full complexity of the problem. The complexity of the problem and the limitations of the EBP approach, together with the more sophisticated tools nowadays available to reproduce the Aeolian vibrations phenomenon are reported in [1][2][3][5] to which we make reference for more details.

However, from the engineering point of view, the EBP is a very useful tool for the design of damping system necessary to control Aeolian vibrations.

2. Analytical methods and assumptions used in the study

The study was carried out by comparing the results of EBP calculations coming from three different experts. All experts based their calculations on the same data sets describing the characteristics of the spacer-dampers, however there were nominal differences in analytical procedures, such as the wind power input functions, self-damping models applied in the EBP calculations, or the modelling of the effects of wind turbulence. Table I summarizes these similarities and differences taken as main assumptions in the simulations. Although the above differences, all the models are based upon the same assumptions and they are developed in the frequency domain, hence a preliminary evaluation of the bundle natural frequencies and modes of vibration is necessary [1][2]. To do this, for each mode of vibration the Aeolian vibration amplitudes are achieved through a balance between the power input from the wind, the power dissipated by the conductors and the damping devices (spacers and dampers).

In all the models the following assumptions are considered:

- The vertical and horizontal components of the conductor motion are taken into account The wind power input is only related to amplitudes in the vertical plane [6];
- The conductor self-damping is due to amplitudes resulting from vertical and horizontal motion;
- The spacer-dampers are modelled through their inertial,

elastic and damping characteristics, as detailed in Table III. The coupling among sub-conductors is defined by the spacer dynamic response, which is a function of the vibration frequency;

- The aerodynamic damping related to the horizontal motion is not considered;
- The torsional stiffness of the conductor is not considered in the computation of the bundle natural frequencies;
- The longitudinal motion is not considered;
- The energy input from the wind comes from wind tunnel tests on two vibrating cylinders, with one in the wake of the other [5][6][7]:
  - Half of the overall energy derived from the wind tunnel tests on two cylinders is applied to any conductor of the bundle (independently on the sub-conductors number)
  - Because the energy is a function of the amplitude of motion of the conductor, each sub-conductor may have different wind power input.

In the following a brief description of the three models considered is provided.

Krispin Model

The computational model determines vibration modes of the conductor bundle [11]. For that purpose, the subconductors are assumed to behave like strings with small bending stiffness. The subconductors are divided into subspans at the locations, where spacers are attached. The spacers are represented by an impedance matrix which describes the relation between the conductor forces and velocity at the spacer clamps. Stockbridge dampers are treated analogously.

Formulating the equation of motions of the subspans and taking into account boundary conditions (clamped span ends) and compatibility conditions at the spacer clamps, leads to a set of homogeneous equations. Solving

		Analytical Methods		
		Diana et al	***Krispin***	***Cosmai (Claren)***
Case data	AA+AE B.	Table II	Table II	Table II
Spacer Characteristics	AA+AE B.	Table III	Table III	Table III
Wind Power Data	AA B.	Curve b Table IV [8]	Curve b Table IV [8]	
	AE B.	Table IV [7][8]	[11], [13]	Curve b Table IV [8]
Consider Turbulence		YES [7][8]	NO	YES (Variable turbulence)
Self-Damping Data	AA B.	Table IV	Table IV	
	AE B.	[10]	[11], [13]	[10]
Calculation Method		[10]	[11], [13]	[10]
Approach		Matrix transfer method. Modal approach	Complex Eigen-modes	Matrix transfer method. Modal approach
Consider Flexural Stiffness		0.5 EJmax	0.5 EJmax	0.5 EJmax
Tensile load differentials	AA B.	No	No	
Tensile load differentials	AE B.	Yes	Yes	No
Energy Balance domain		Single Freq	Single Freq	Single Freq
Spacer Model		[10]	[11], [12]	[10]
Possible to Consider Dampers		Yes	Yes	Yes
Possible to Consider Armour rods		Yes	No	Yes

Table I - Analytical Methods and Assumptions Used in the Study (Numerical table entries refer to supporting references)

Note: AA B. stands for Analytical-Analytical Benchmark, while AE B. stands for Analytical-Experimental Benchmark.

the eigenvalue problem gives the complex eigenvalues. The corresponding eigenvectors define the complex eigenmodes.

The EBP method is employed to evaluate the vibration amplitude of these modes. Complex mode shapes have antinode and node amplitudes that vary along the span. The complex mode shape is approximated by an equivalent standing wave possessing the same mechanical energy as the complex wave. Conductor self-damping and wind power input are evaluated for the amplitudes of this equivalent standing wave. Power dissipation of the spacers is derived from the clamp velocities and the spacer impedance.

Vibration intensity is calculated in terms of the maximum value of $.Y_{max}$, which is the product of frequency and antinode amplitude in the respective subspan. Nominal strains at clamping points are derived by using well-known relationships between nominal strain and $.Y_{max}$.

Diana Model:

In this model, eigen frequencies and eigenmodes of the system (real modes) are computed through the matrix transfer method. Field matrices $[B_i]$ (i=1,..,N with N=number of subspans) defining the relationship between displacements and forces on the conductors at the extremities of each subspan and point matrices $[P_j]$ (j=1, ….,N-1) defining the relationship between displacement and forces on the conductors right side and left side of each spacer are defined. The product of all the field and point matrices, gives a matrix [A] defining the relationship between displacements and forces at the span extremities. End conditions allow for the computation of the eigen frequencies and correspondent eigen modes [7,8,9,10]

Hence in the Diana model the EBP is applied for each computed eigenfrequency/eigenmode considering both the energy introduced by the wind and the one dissipated by the system.

All the damping sources, such as spacers dampers and, cables are accounted for. For the eigenfrequencies and eigenmode where the amplitude of oscillations are not zero, the amplitude of motion and the resulting deformations are computed. Moreover the model allows to account for frequency dependent spacer stiffness and damping and tension differential between bundle conductors.

Finally the main outputs of the model consist in:

- The maximum amplitude of oscillation over the whole span;
- The maximum amplitude of oscillation registered in correspondence of spacer and damper clamps over the whole span
- The strain in correspondence of singularities of the system: i.e at the suspension clamp, at the armour rods and at the spacer and damper clamps;

It must be pointed out that the matrix transfer method, applied to the above described approach, has been also applied to the models developed in Russia for vibration of single [14,15] and bundle conductors.

Claren - Cosmai Model:

This model [8] [10] is the same as the Diana model, using the same software.

However during the years some changes have been introduced in the formulation of the energy dissipated by the conductors and of the energy introduced by the wind.

3. Benchmarks

In this section the results obtained for two different benchmarks are summarised: the first one is an analytical-analytical benchmark, i.e. the amplitudes and strains predicted by the various available models applied to a certain test case are compared; the second one is an analytical-experimental benchmark: in this case strains predicted by analysis are compared to strains actually measured in a field test in Pakistan. The experimental data were available to the benchmark participants since the beginning. In table II the main information concerning the considered experimental tests are reported, while table III summarises the spacer data The input data of tables II and III are used by both the benchmarks.

In order to provide comparable results and highlight the main differences in the models, the same energy input from the wind and the same dissipated energy for the conductors have been introduced in the analytical-analytical benchmark (see table IV).

Analytical – Analytical benchmark results:

For the analytical-analytical benchmark the two considered models are the ones of Krispin and Diana, both of them

Characteristics of the Test Span – Section 1 (Tarbela-Jalapur-Sharif)	
Location	Between towers 443-444 (susp - susp)
Span length (l) [m]	449
Terrain condition	Broken area, open terrain with low vegetation
Elevation above sea level [m]	494
Number of circuits	1
Phase configuration	Quad bundle, 457mm separation
Phase conductor	
Type and name	ACSR Drake
Diameter (D) [mm]	28.14
Mass per unit length (m) [kg/m]	1.628
Ultimate Tensile Strength (UTS) [N]	139060
Tensile load (T) [N]	32000
Stranding	7 steel wires + 26 aluminum wires
Elementary wire diameters [mm]	3.45 (steel) - 4.44 (aluminum)
Spacer damper	
Number	7
Subspan lengths [m]	37 – 63 – 55 – 68 – 61 – 69 – 59 - 37

Table II – Experimental tests characteristics and system configuration data

use the same functions for wind power and conductor self-damping as shown in Table IV; it is then easier, from the results, to highlight the structural differences in the models.

The Claren-Cosmai model is not considered for this type of benchmark, because it should provide exactly the same results as the Diana model.

The predicted maximum vibration amplitudes for each mode of vibration are reported in figure A.2 - as a function of frequency - for the Diana and Krispin model. The predicted maximum strains are reported in figure A.3.

In both the cases the same tensile load is applied on the conductors of the bundle and a constant low wind turbulence is imposed, according to Table I and table IV.

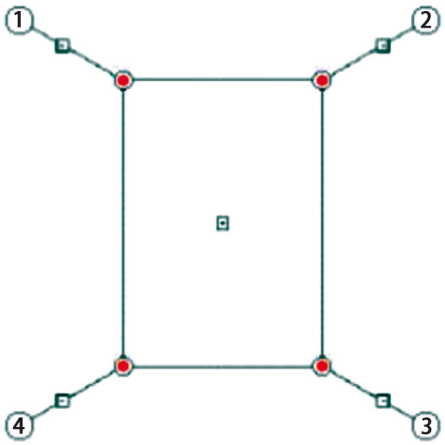

Central body mass	2.177	kg
Arm mass	0.735	kg
Central body Moment of inertia	6.47 10-2	kg m2
Arm Moment of inertia	1.57 10-3	kg m2
Hinge torsional stiffness KT	333	Nm/rad
Torsional loss factor	0.35	HT/KT
Hinge axial stiffness KA	100	kN/m
Axial loss factor	0.2	HA/KA

Table III – spacer-damper data

Wind Power Input	**Conductor Self-damping**
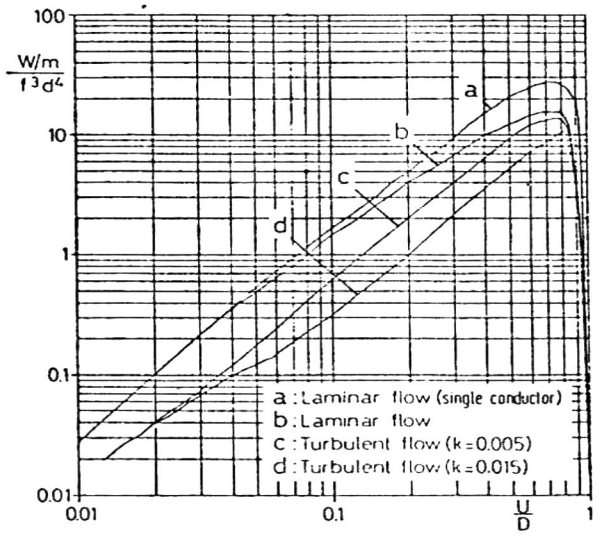	**W/l = power dissipated per unit length of conductor [W/ m] W/l = DC U² f⁴** l = span length [m] U = vibration amplitude [m] f = vibration frequency [Hz] conductor data: m = mass per unit length = 1.628 kg/ m; T = tensile load = 32000 N; D = diameter = 0.02814 m DC = damping constant = 0.003089
Curves b,c,d are wind power input curves on each one of the bundle conductors, for different turbulence levels. Te wind power input used in the analytical-analytical benchmark is that represented by curve 'b', corresponding to low turbulence ($I_t < 0.07$)	Conductor self-damping used for the "analytical-analytical" benchmark

Table IV – wind power input and conductor self-damping for the analytical-analytical benchmark

In figure A.2:

- the continuous lines, reported for reference purpose, show the results obtained in the case of a single conductor at the same tensile load of the bundle conductors (the blue line refers to Diana Model, the red one to Krispin model),
- the blue diamonds (Diana) and red crosses (Krispin) represent the maximum amplitude observed on the bundle conductors.

The diagram shows that, even if there are some differences in the two models, the trend in the results is very similar.

As far as the maximum strain is considered, figure A.3 shows the bundle maximum strain both in correspondence of the spacer clamp (green triangles and red diamonds) and the suspension clamp (violet triangles and blue diamonds), for Krispin (triangle points) and Diana models (diamonds points).

Also in this case, for the whole range of frequency considered, a general good agreement between the results can be observed. There is a good agreement between the two model results for frequencies up to 25 Hz, while at higher frequencies, where the amplitude of vibration for both the models are very low (see figure A.2), the Krispin model shows a level of strain higher than the one of Diana.

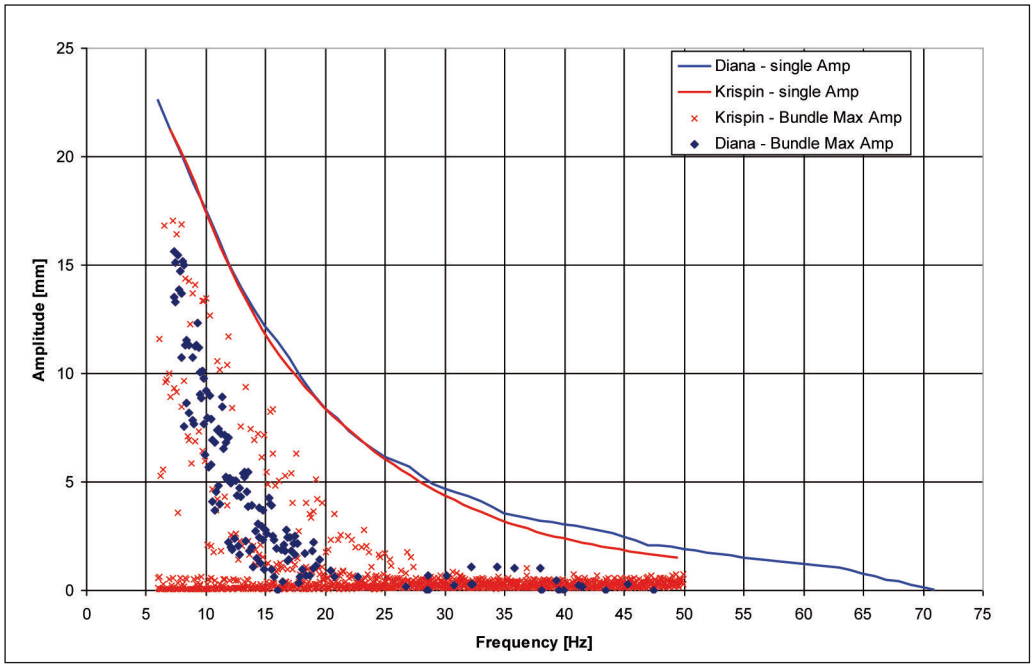

Figure A.2- Predicted maximum Aeolian vibration antinode amplitude (0-peak) as a function of frequency when the same tensile load is applied on the subconductors and a constant low wind turbulence is considered

Analytical – Experimental benchmark results

In the analytical-experimental benchmark the models - described in section 2 - use for the wind power input and conductor self-damping their own selected function, as shown in Table I.

Moreover, the data describing the field span and the spacer are the same as for the analytical-analytical benchmark (table II and III).

The experimental results for the test case are available in the form of strains (0-peak value) at the suspension clamp, deduced by bending amplitude measurement performed through a typical vibration recorder.

Experimental and numerical results are compared, for the different models, in figures A.4, A.5, A.6 when the same tensile load is applied to each sub conductor and a constant low turbulence is considered. The choice of a low turbulence level is related to the terrain description given in Table II.

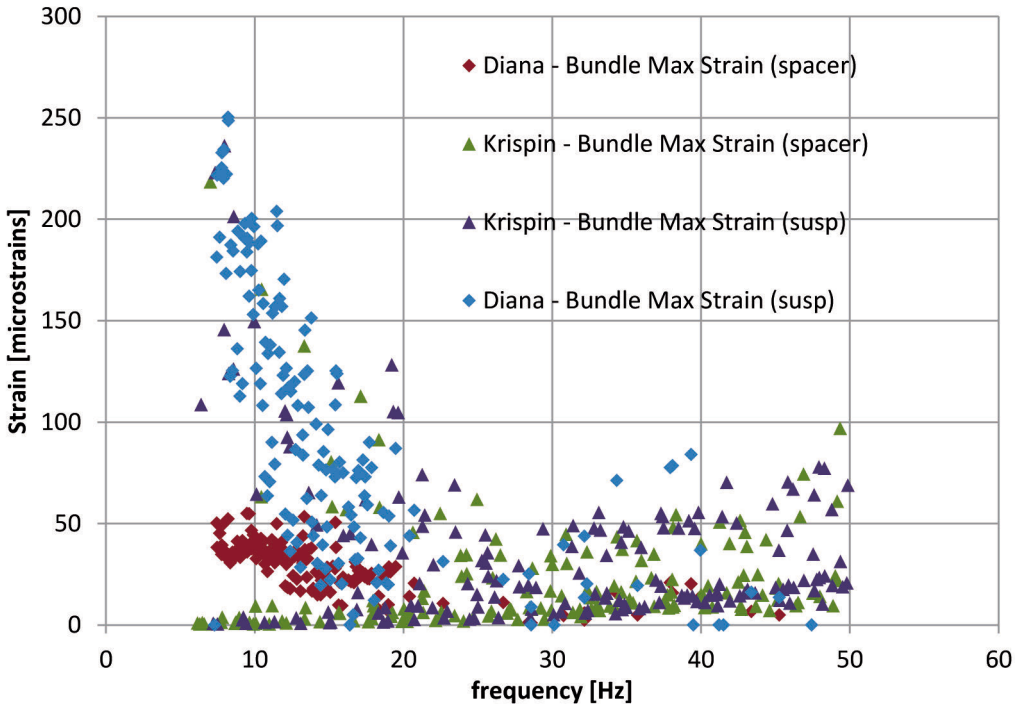

Figure A.3 - Predicted maximum strain (0-peak) on the bundle conductors at the suspension clamp and at the spacer clamp as a function of frequency

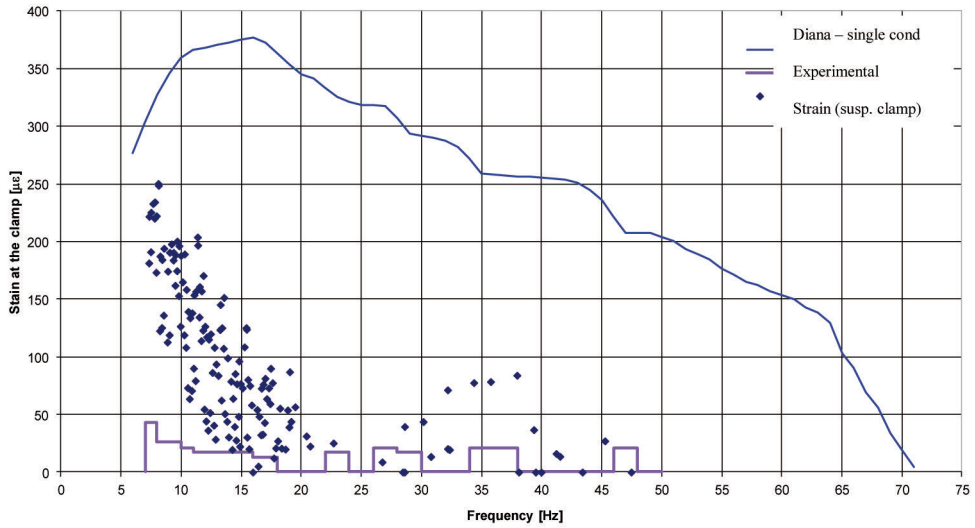

Figure A.4: Maximum strains at the suspension clamp with the Diana model : when the same tensile load is applied to the subconductors of the bundle and a constant turbulence (It < 0.07) is considered

Figure A.4 shows the maximum strain for the bundle conductors in the case of the Diana model. It can be seen that, when the same tensile load is applied on the subconductors and a constant low wind turbulence index It lower than 0.07 is considered, the numerical data are conservative with respect to experiments in the frequency range 5-20 Hz.

In figure A.5 the same analysis described for figure A.4 is replicated using the Claren-Cosmai model. As expected, the results appear to be similar to the one obtained by means the Diana Model

The two considered turbulence levels (It < 0.07 and It = 0.05) have to be considered equivalent, representing the lowest turbulence levels present in each of the two computation programs.

Finally, the same analyses as before are replicated by means of the Krispin model. As it can be seen, the numerical results are still conservative and similar to the previous ones.

In order to achieve a better understanding of the discrepancies highlighted before between experimental and numerical results, a sensitivity analysis (figure A.7, A.8, A.9, A.10) has been performed, within the benchmark. Two main factors have been considered: the first is the wind turbulence, that is generally not constant with the wind speed, the second is that the tensile load cannot be exactly the same on all the bundle subconductors. It's a practice in the bundle design to string the bottom conductors with a lower tensile load with respect to upper ones. Hence the modes of vibration will be affected by this tension differential [12]. The tension differential is expressed in terms of difference in sag, measured in conductor diameters (D): sensitivity analysis has been done considering a 1D and a 10D situation.

As a first step the influence in the results of variable wind

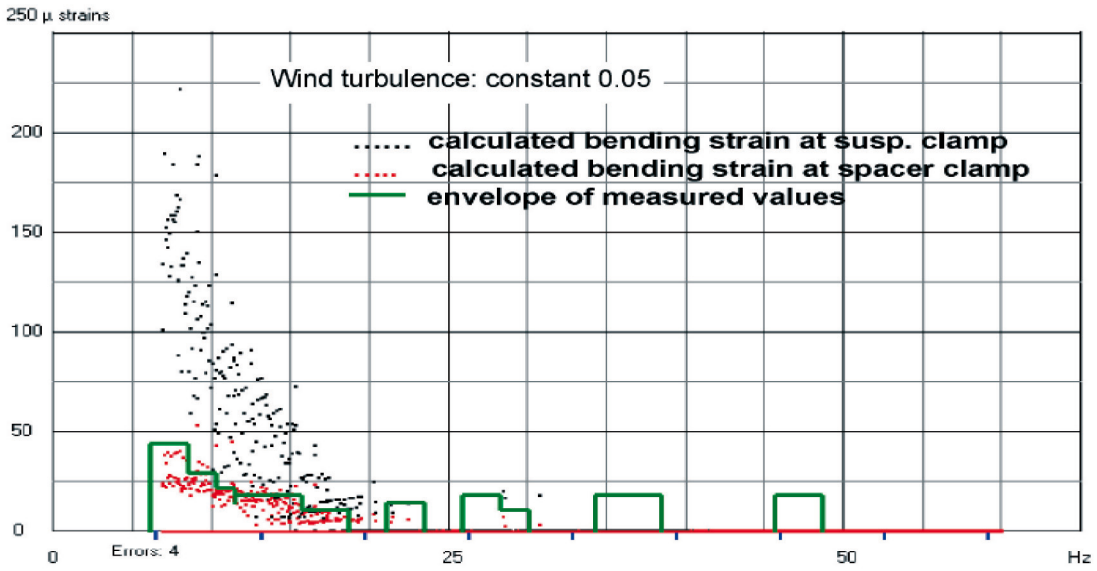

Figure A.5: Maximum strains at suspension clamp with Claren-Cosmai model : when the same tensile load is applied to the subconductors of the bundle and a constant turbulence (It = 0.05) is considered

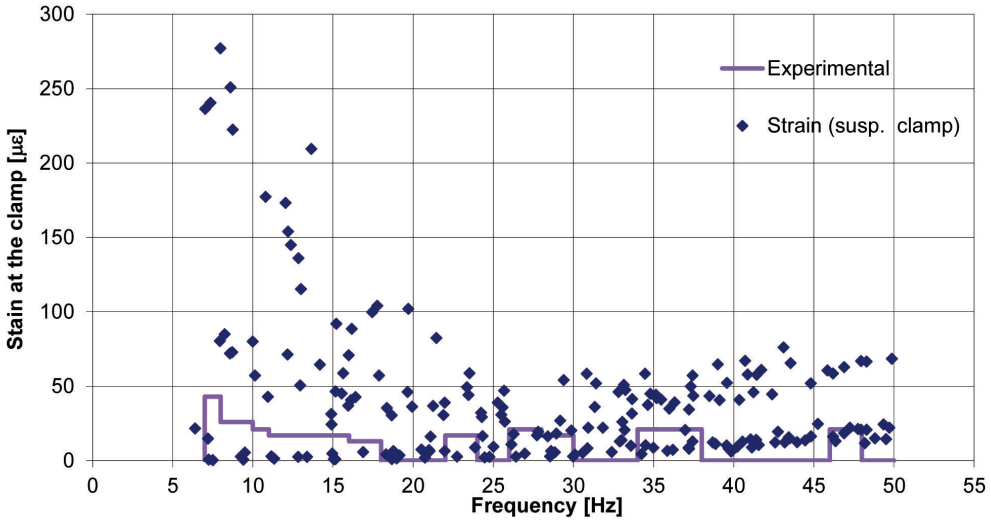

Figure A.6: Maximum strains with Krispin model : when the same tensile load is applied to the subconductors of the bundle and a constant, low, wind turbulence is considered

turbulence is considered: a typical trend (black points) of measured turbulence as function of wind speed is reported in figure A.7[1]: the continuous line represents the index of turbulence as function of speed considered in the Claren-Cosmai model.

Figure A.8 reports the numerical maximum strains at the suspension clamp when the above described variable turbulence is considered (figure A.7): it is evident that the maximum strains undergo a reduction of around 75% with respect to the ones presented in figure A.5, and show a good agreement with the experimental findings.

The influence of tension differential has been also investigated, using the Diana model (see figure A.9 and A.10).

In figure A.9 the maximum strains at the suspension clamp are reported when a 1D tension differential is applied to the bundle. The application of a tension differential always leads to a strain decrement in the bundle: it can be seen that the decrease of strain level when a 1D tension differential is applied is low.

Finally, in figure A.10 the maximum strains at suspension clamps computed considering a tension differential of 10D is reported. Moreover in this calculation the variation of stiffness and damping with respect to frequency for the spacer has been considered. It can be observed that in order to achieve level of strain close to the experimental one, a tension differential of 10 D is required. This tension differential expressed in conductor diameters (10 D) corresponds to a percentage tension differential between upper and lower sub-conductors of the order of 2%.

4. Conclusions and future work

The two benchmarks assessed within the Working Group allowed to understand the main differences among the

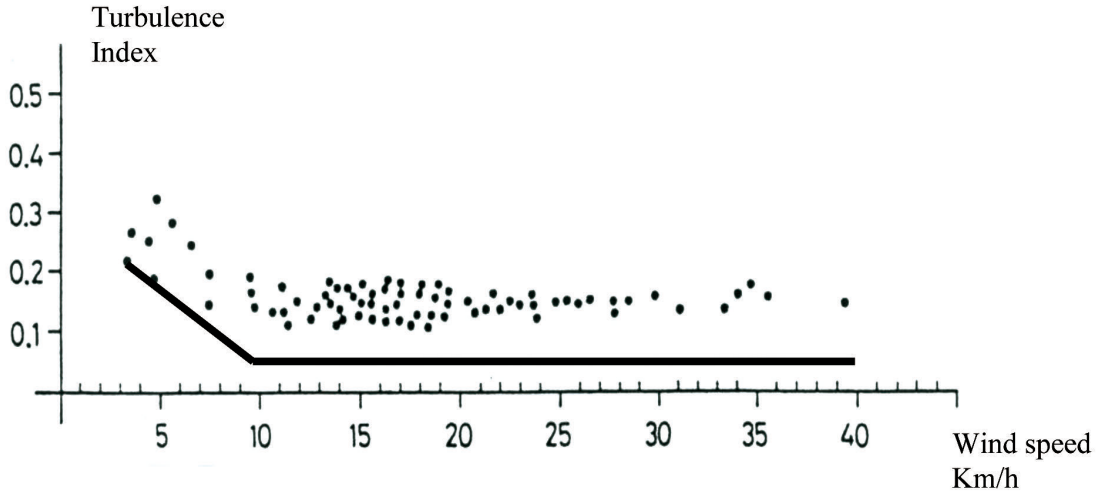

Figure A.7 Cosmai hypothesis for variable wind turbulence index

[1] - The measured turbulence index (black points) in fig A.7 is not that measured in the site to which the field measurements of the AE Benchmark refer. It only represents a typical trend of turbulence index, not related to a very flat terrain, showing that at low wind speeds, generally, turbulence increases as the wind speed decreases.

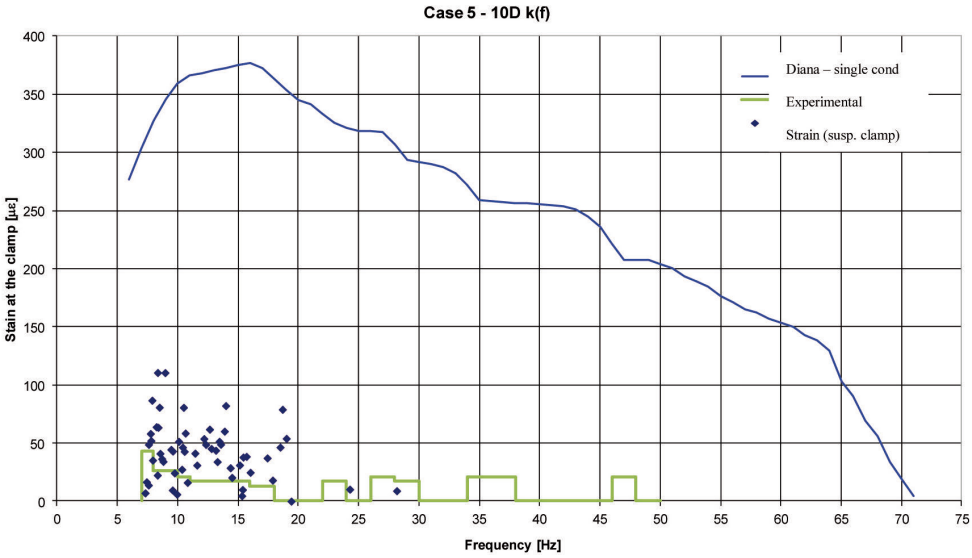

Figure A.8: Maximum strains at suspension clamp with the Claren-Cosmai model : tension differential neglected and variable turbulence (0.20 < It < 0.05) considered

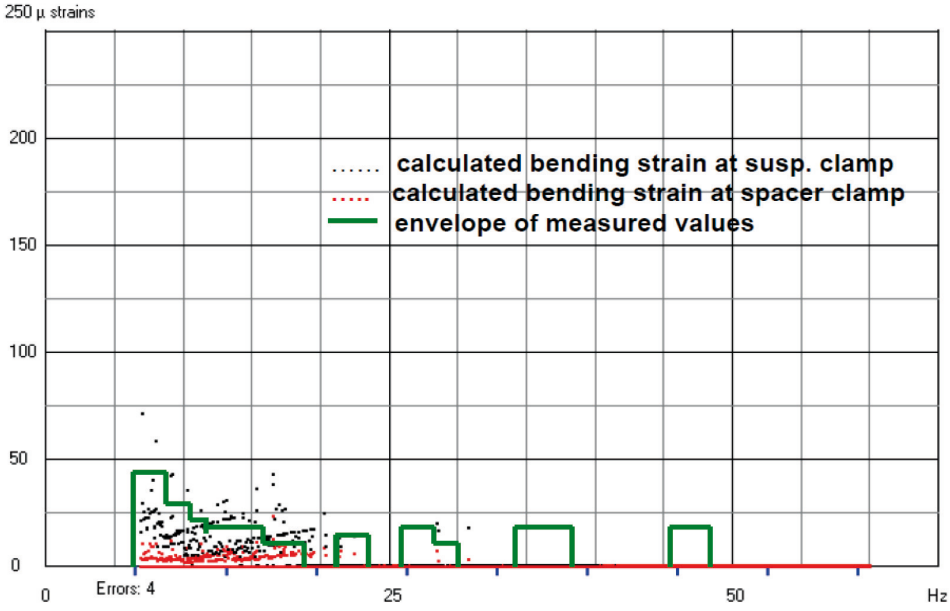

Figure A.9 Maximum strains at suspension clamp with the Diana model : tension differential 1D and constant turbulence (It < 0.07) considered

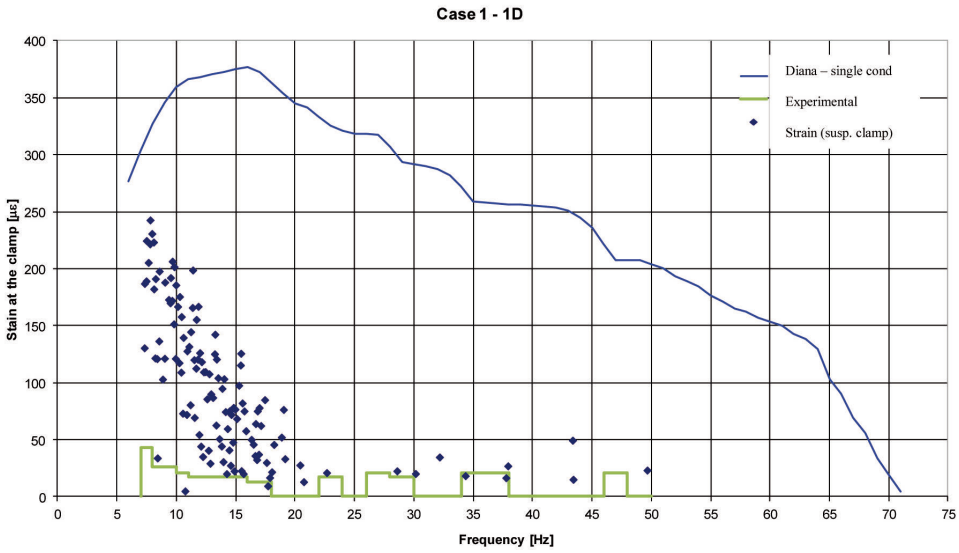

Figure A.10: Maximum strains at suspension clamp with Diana model : tension differential 10 D and constant turbulence (It < 0.07) considered

models presently adopted in the field of cable vibrations to understand and prevent Aeolian vibration.

The analytical – analytical benchmark showed that the computed vibration have a very similar trend even if some differences in the models are present.

As far as the experimental-numerical benchmark, the numerical results generally exceed the experimental ones and then they are conservative, at least at low frequencies.

The benchmark has been developed on one case only, considering a quadruple bundle: this is of course a limitation and future work comparing analytical – experimental results from different cases (different bundle configurations and different conductors) should be planned.

In any case, it is needed to point out that, generally, when dealing with twin bundles, numerical results appear to be less conservative in respect to the experimental data [4][7].

The sensitivity analysis demonstrated that a non-negligible influence in the assessment of cable behaviour, when dealing with Aeolian vibrations, is given by the introduction of tension differentials and variable wind turbulence with wind speed.

Clearly it is not straightforward knowing the real value to assign to the turbulence and to the tension differentials when the bundle behaviour for Aeolian vibrations must be analysed.

Future work to achieve better knowledge on this issue should consider comparison between measurements on a real line and analytical results.

5. References

[1.] *CIGRE TF 22,11,01, "Modelling of Aeolian vibration of Single Conductors - Assessment of Technology". Electra 1998 – N.181*

[2.] *CIGRE TF B2,11,01, "Modelling of Aeolian vibration of a single conductor plus damper: assessment of technology". Electra 2005 - N.223*

[3.] *CIGRE WG B2.31, "Modelling of Aeolian vibration of single conductors strung at relatively high tensile load. Application to HV & UHV lines", Electra 2011 - n.256*

[4.] *CIGRE TF B2.11.04, Technical Brochure 273 – 2005, "Overhead conductor safe design tension with respect to Aeolian vibrations"*

[5.] *G. Diana, M. Falco, M. Gasparetto , "On vibrations due to vortex shedding induced on two cylinders with one in the wake of the other". Meccanica, n.3, 1976*

[6.] *D. Brika, A. Laneville, "The Power Imparted by Wind to a Flexible Conductor in the Wake of Another", IEEE Power Engineering Review, Vol. 17, No. 1, 1997.*

[7.] *Belloli, M., F. Resta, D. Rocchi, and A. Zasso, "Wind Tunnel Investigation on Aeroelastic Behaviour of Rigidly Coupled Cylinders." Proc. 5th Int'l Symposium on Cable Dynamics. Santa Margarita Liguria (Italy). September 15-18 2003*

[8.] *G. Diana, M. Gasparetto, F. Tavano, U. Cosmai, "Field measurement and field data processing on conductor vibration (comparison between experimental and analytical results)". CIGRE' International Conference on Large High Voltage Electric Systems, 1982 Session*

[9.] *G. Diana, G. Di Giacomo, R. Claren , "An approach to vortex shedding under turbolent air flow on a single vibrating cylinder". IEEE 1979 Summer Meeting, July 15, N.Y*

[10.] *R. Claren, G. Diana, F. Giordana, E. Massa , "The vibrations of transmission line conductor bundles". 71 TP 158 PWR - IEEE Winter Meeting, 1971*

[11.] *K. Anderson, P. Hagedorn , "On the energy dissipation in spacer-dampers in bundled conductor of overhead transmission lines". Journal of Sound and Vibration, 180(4), pp. 539-556, 19Verma, H. - "Aerodynamic and structural modeling for vortex-excited vibrations in bundled conductors". Doctor's thesis, Darmstadt, 2008*

[12.] *Foata, M., Noiseux, D., "Computer Analysis of Asymmetries of a Two-Conductor Bundle upon its Aeolian Vibration", IEEE Trans. on Power Delivery, Vol. 6, No. 3, July 1991*

[13.] *T. Hadulla, "Vortex-induced vibrations in overhead line bundles". Doctoral Thesis, Technische Universität Darmstadt, 2000*

[14.] *O. Afanasyeva, S. Ryzhov, V. Feldshteyn "Dynamic models for the study of vibration Power Line conductors and communication cables in the air flow" Problems of Mechanical Engineering and Automation, 1998, No 1, pp. 50 – 57*

[15.] *O. Afanasyeva, V. Feldshteyn, S. Ryzhov, "Calculation of rational geometry of the helical support clamp under the terms of vibration", Electricheskie Stantsii (Power Plants) 1998. No 1, pp. 12 – 17*